



ELSEVIER

Journal of Power Sources 97–98 (2001) 181–184

JOURNAL OF
**POWER
SOURCES**

www.elsevier.com/locate/jpowsour

Sn–Ca amorphous alloy as anode for lithium ion battery

L. Fang^a, B.V.R. Chowdari^{a,b,*}

^aInstitute of Materials Research and Engineering, Singapore 117602, Singapore

^bPhysics Department, National University of Singapore, Singapore 119260, Singapore

Received 16 June 2000; accepted 31 December 2000

Abstract

Amorphous Sn–Ca alloys were synthesized by solution technique using NaBH₄ as the reducing agent. The particles are found to be homogeneous with size ~4 µm. The alloys were tested using Li metal as counter electrode. The capacity has been found to be 400 mAh/g and 62% of it was retained after 70 charge–discharge cycles. The ex situ XRD technique was used to illustrate the progress of Li intercalation. Cyclic voltammograms show that the two peaks located at 0.6 and 0.2 V, respectively, correspond to the charge and discharge plateaus. The observation of voltage plateau at about 1.0 V confirms the formation of solid electrolyte interface (SEI) on the surface of the anode. The intercalation of Li is through the formation Li₅Sn₂ phase, which was confirmed by HRTEM. © 2001 Elsevier Science B.V. All rights reserved.

Keywords: Sn–Ca amorphous alloy; Charge–discharge; Lithium ion battery

1. Introduction

The commercialization of lithium ion batteries by Sony in 1990 has resulted in extensive investigations of various cathode and anode materials. Efforts have been made to improve the limited capacity exhibited by graphite anode (372 mAh/g). One of the interesting systems that have been studied is tin containing material, which includes tin alloys and amorphous tin composite oxides (ATCO) with a capacity as high as 600 mAh/g [1]. ATCO contains Sn(II)–O as active center for lithium reaction which is reduced to tin metal and, subsequently, forming an alloy with lithium in charge–discharge process [2,3]. During the first discharge process with Li metal as cathode, part of Li reacts with oxygen in SnO to form Li₂O and this causes initial large irreversible capacity loss.

Tin alloy anode materials such as Li–Sn, Sn–Fe, Mg₂Sn, Sn–Cu, etc. have been studied in recent years [4,5,6]. The main problem concerned with these is the capacity fading due to large volume change which occurs during charge–discharge cycling. Hence, the ideal anode should contain Sn nano-crystallites since there will be no need to convert SnO to Sn and no initial capacity loss due to formation of Li₂O. But the main challenge is to overcome large volume change during cycling which introduces stress and strain. One

possibility to reduce large strain and stress is to use materials in the amorphous or glassy state. Another way is to choose a matrix, which has low elastic modulus and can absorb large stress and strain during cycling. In fact, carbon is well known for its low elastic modulus (18.1 G N/m²) [7] and is used as anode in the state-of-art lithium ion battery. Calcium metal also exhibits low elastic modulus (19.6 G N/m²), and hence, it is selected as the matrix material for the present study.

In order to obtain dispersed fine powders of the Ca–Sn metal alloy, the method of the sodium borohydride reduction in aqueous solution has been used [8]. The advantage of this method is that the process is simple and fast. The alloys with different structural arrangements, such as amorphous, nano-crystallite mixed with amorphous, etc. can easily be obtained by varying the synthesis conditions. Sodium borohydride is thermodynamically unstable in aqueous solution. However, provided the solution is maintained at pH of 2–5, a short kinetic stability window is available for reduction chemistry. It has been found that drop wise addition of sodium borohydride to rapidly stirred solutions containing Ca²⁺ and Sn²⁺ produces precipitates of fine particulate Sn–Ca amorphous alloy.

2. Experimental

Reagent-grade SnCl₂ and CaCO₃ were used as supplied by Aldrich. The composition is prepared according to Sn:Ca

* Corresponding author. Tel.: +65-8742956.

E-mail address: phychowd@nus.edu.sg (B.V.R. Chowdari).

ratio 1:1. Dilute solutions of Sn:Ca (0.01 mol) were prepared in 500 ml distilled water. A series of solutions with pH value from 3.0 to 11.0 were prepared by adding NaOH solution (32%). Reducing agent solution (NaBH_4 2 M) was prepared by dissolving NaBH_4 in distilled water with pH value 11. The reducing solution was added drop wise into the Sn:Ca solution stirred by magnetic bar at room temperature. The precipitate formed immediately and the whole process takes only several minutes. The precipitates were washed several times with distilled water to remove chlorine and residual carbonate. The particle size was measured by the particle size analyzer (Elzone 5380, Micromeritics, USA). Electrodes of the material were prepared by coating onto a copper foil, slurries of the respective powder, Super S carbon black and PVDF in the weight ratio (80:5:15) dissolved in NMP solvent. The electrode was dried in oven and roller-pressed and then cut into 1.6 cm diameter discs. The coin cell (2416) was fabricated in an Ar-filled dry box (MBraun) using a polypropylene micro-porous separator, an electrolyte (1 M LiPF_6 dissolved in EC and DMC) and lithium foil (1.5 cm diameter) as the counter electrode. All cells were tested with a constant current of 50 mA/g and were charged and discharged between 0.1 and 1.2 V.

Ex situ XRD was used to characterize the crystal structure of the materials under different discharge level. The electrode was taken out from the test cell discharged to different state and sealed in a polyethylene terephthalate film (PETP) for experiment. This process was done in the glove box. Samples for HRTEM were prepared from the powder taken from the cells discharged to respective voltages. The powder was washed by NMP solvent several times and followed by dispersing in collodion solution (2%). The solution was then dropped on to the clean water surface to form thin film which was then transferred to a TEM grid, followed by carbon coating. The XRD and HRTEM experiments were done using a Philips diffractometer (PW1710) with $\text{Cu K}\alpha$ radiation ($\lambda = 1.5405 \text{ \AA}$) and a Philips field emission electron transmission microscope (CM300), respectively.

3. Results and discussion

3.1. Synthesis and characterization

Synthesis condition is critical to the final products and pH value plays an important role. While a solution of $\text{pH} < 4$ tends to form fully crystallized alloy phases, a solution with pH between 5 and 6 yields relatively less-crystallized powder. Hence, amorphous alloy powder was prepared using dilute solution at pH value about 6.5. XRD data have shown that most crystallized samples are of one phase identified as Sn crystallite of space group $I\bar{4}_1/\text{amd}$. The XRD peak intensities of Sn are found to decrease with the reducing amount of NaBH_4 . The molar ratio of NaBH_4 to starting material is <0.25 and the amorphous alloy is obtained with concentration of solution <0.001 mol.

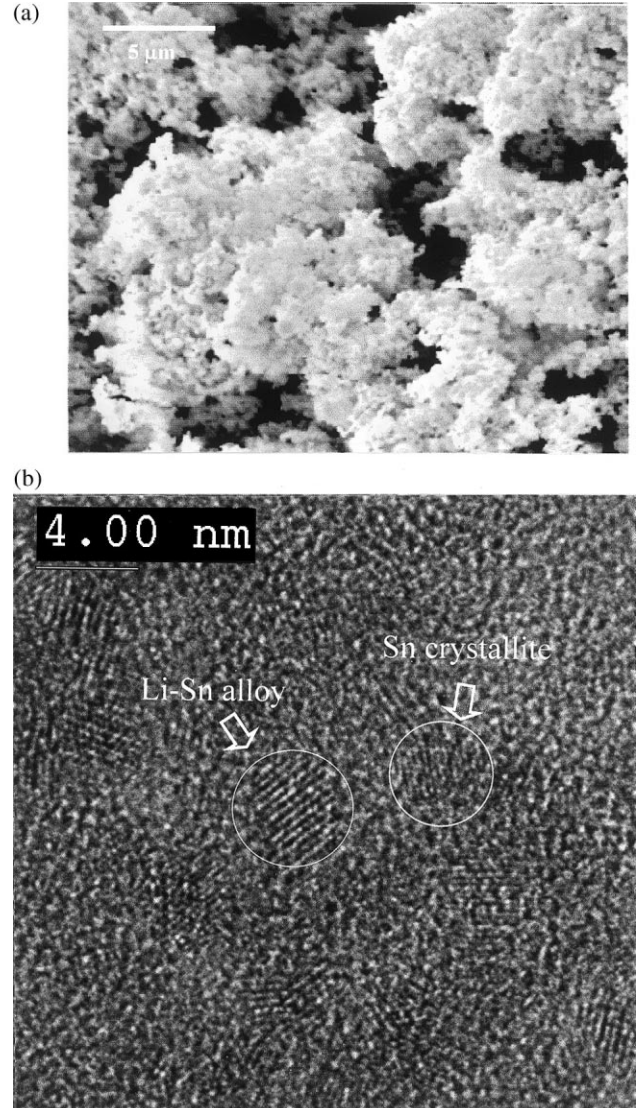


Fig. 1. (a) SEM micrograph of Ca–Sn amorphous sample; (b) HRTEM micrograph of Ca–Sn amorphous sample discharged to 0.4 V after five complete cycles.

Since the materials are synthesized by chemical solution reducing method, the particles obtained here have very fine size and narrow size distribution. The typical size distribution presents a Gaussian shape with the maximum located at $4.2 \mu\text{m}$ and FWHM about $0.7 \mu\text{m}$. Fig. 1a presents the morphology of one of the samples which shows that all particles are agglomerates of smaller ones. The density of the sample is about 4.32 g/cm^3 , which was measured by a Pycnometer (Acupyc 1330, Micromeritics, USA) using helium as the displacing media.

To study the reaction process that occur in the amorphous Sn–Ca alloy, an ex situ XRD experiment was carried out. The cells were run for two complete cycles to a fully charged state and followed by discharge to 1.0, 0.5 and 0.1 V, respectively. Fig. 2 shows the XRD patterns of respective discharge states. The material as prepared shows

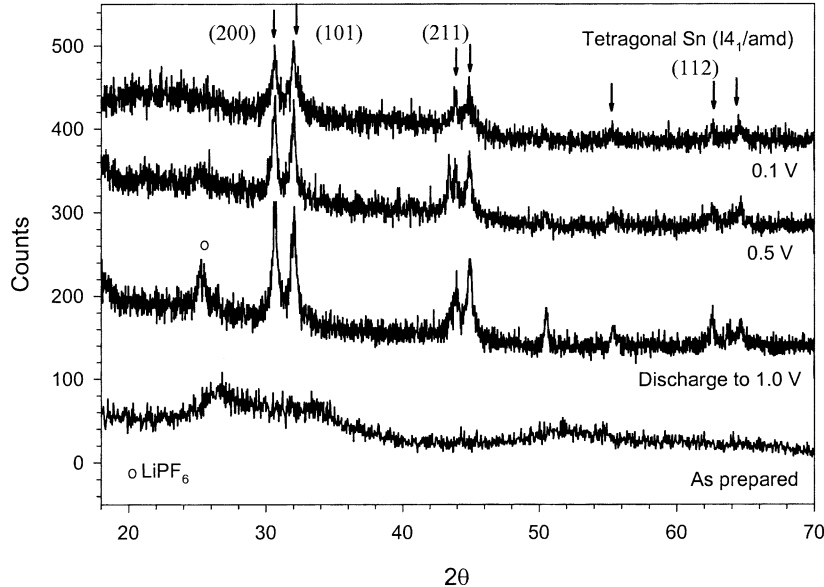


Fig. 2. Ex situ XRD patterns of the amorphous Ca–Sn materials. The XRD patterns are obtained on the samples discharged to corresponding voltage after two complete cycles.

an amorphous state. As the cell is discharged to 1.0 V, two main peaks appeared at 2θ , 30.27 and 31.82°, which indicates the formation of tetragonal Sn crystallites. The Sn crystallites have the structure of I4₁/amd (1 4 1) and corresponding *a* and *c* lattice parameters are 5.83 and 3.18 Å, respectively. The cells discharged to low voltages showed a decrease in the peak intensity. In Sn containing composite anode, the reaction mechanism of Li-intercalation is through the formation of Li–Sn alloy accompanying the consumption of Sn crystallites. But no peaks were indicated for the presence of Li–Sn alloy in our samples. This phenomenon has been understood only after HRTEM experiment was done.

Fig. 1b shows the sub-microstructure of the material (HRTEM lattice image) discharged to 0.4 V. The crystallites can be identified from the lattice image. One with relatively large inter-planar distance is confirmed to be Li_5Sn_2 crystallite and the other with small inter-planar distance is the tetragonal-Sn particle. It is noticed that all Li_5Sn_2 crystallites are around 5 nm in size and this is the reason why no evidence for the formation of Li_5Sn_2 alloy could be obtained from XRD pattern. TEM micrograph shows that all Sn and Li_5Sn_2 crystallites are well distributed in the amorphous matrix and all particles form a network. Such structure is ideal for an alloy anode, as we know that most alloys have quite large volume change between charged and discharged states. Real nano-size of Li_5Sn_2 effectively enables the lattice strain distributed evenly in the matrix. However, most crystallized samples will have Li–Sn alloy crystallites larger than 100 nm and this causes the strain concentrated locally during cycling. Sub-microstructure and choice of matrix for alloy anode materials is very important. In a discharge cycle, Sn transforms to Li_5Sn_2 with an volume expansion 2.86 times and in a charge cycle the volume will shrink to about

one-third [9]. Now the question is what will happen if the matrix does not have a proper stress and strain property. The intercalation of lithium will be limited to some extent if the elastic modulus is too high and reversible capacity cannot be fully recovered if the elastic modulus is too low. Especially the capacity will fade fast when the strain goes over the elastic region and some residual strain will be kept. This means there will be a gap between the matrix and Sn active center and definitely this will cause fast capacity fading.

3.2. Electrochemical characteristics

Typical cyclic voltammograms of alloy anodes are shown in Fig. 3a. The scan rate of the voltammogram is 0.3 mV/s in the potential range from 0 to 1.2 V at room temperature. The first cycle is different from the subsequent cycles and the main difference is that it has a plateau at 1.0 V (Fig. 3c), which is due to the formation of solid electrolyte interphase (SEI) since from the second cycle, the plateau disappeared. The main cathodic peak is located at 0.2 V versus Li^+/Li , with anodic peak at 0.6 V. The subsequent cycles present good reversibility. Lithium ion intercalation and de-intercalation are, therefore, easier after the first cycle. The voltammogram of crystallized sample is similar to that of amorphous sample. The capacity versus cycle number of amorphous sample is given in Fig. 3b and it was found that the capacity of 400 mAh/g could be retained up to 62% after 70 cycles. However, the capacity of crystallized samples was found to fade much faster compared to the amorphous sample. This is probably due to the fact that amorphous matrix is capable to sustain high strain during cycling process. Some samples of Sn–Cu and Sn–Mg alloys were also tested and the capacity of all samples faded very fast

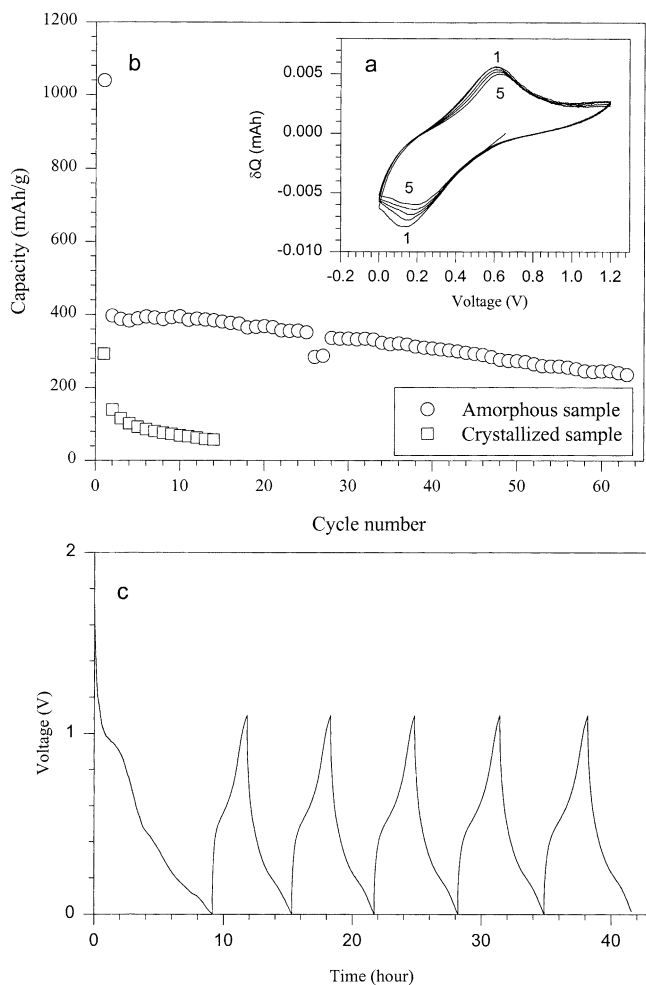


Fig. 3. (a) Typical cyclic voltammogram of amorphous Ca–Sn sample at 0.3 mV/s; (b) capacity vs. cycle number of Li/Ca–Sn cells (1 mA/cm^2 and 0–1.1 V) (active material:super carbon:PVDF = 80:5:15); (c) voltage profiles of amorphous Ca–Sn sample for the first five cycles.

compared to that of the amorphous Ca–Sn alloy. In fact, as seen from the voltammograms of Sn–Mg and Sn–Cu samples, the anodic and cathodic peaks are identical, and hence, the reason for capacity fading is largely related to the matrix. Due to the results that all crystallized alloy samples have serious capacity fading, we believe that amorphous state is more capable to sustain large strain as explained in the

previous section. No grain boundary exists in amorphous material, and hence, easy accommodation of the volume change of the active center without much stress and strain.

4. Conclusions

Nano-size porous Ca–Sn alloy has been synthesized by NaBH_4 solution reducing method. The advantage of using Ca as matrix material is that it can absorb large amount of volume changes. The amorphous state is superior to crystalline state and it is believed that amorphous structure can effectively control the Sn crystallite size in the range of 5–10 nm. The capacity of 400 mAh/g can be retained up to 62% after 70 cycles. The reduced capacity fading in amorphous Ca–Sn alloy is believed to be due to the absence of grain boundaries and low elastic modulus of calcium matrix. Formation of nano-size Li_5Sn_2 crystallites during cycling was confirmed by HRTEM.

Acknowledgements

Thanks are due to Prof. G.V. Subba Rao for stimulating discussions and Dr. H.J. Lindner for his interest in the progress of the work. Thanks are also due to Ms. Doreen Lai for her technical assistance.

References

- [1] Y. Idota, T. Kubota, A. Matsufuji, Y. Maekawa, T. Miyasaka, Science 276 (1997) 1395.
- [2] I.A. Courtney, J.R. Dahn, J. Electrochem. Soc. 144 (9) (1997) 2943.
- [3] S. Machill, T. Shodai, Y. Sakurai, J. Yamaki, J. Solid State Electrochem. 3 (1999).
- [4] R.A. Huggins, Solid State Ionics 113/115 (1998) 57.
- [5] J.O. Besenhard, J. Yang, M. Winter, J. Power Sources 68 (1997) 87.
- [6] K.D. Kepler, J.T. Vaughey, M.M. Tackery, J. Power Sources 81/82 (1999) 383.
- [7] R.C. Weast (Ed.), Handbook of Chemistry and Physics, 67th Edition, CRC Press, Boca Raton, FL, 1986.
- [8] J. Yang, Y. Takeda, N. Imanishi, T. Ichikawa, O. Yamamoto, J. Power Sources 79 (1999) 220.
- [9] M. Winter, J.O. Besenhard, M.E. Spahr, P. Novak, Adv. Mater. 10 (1998) 725.